

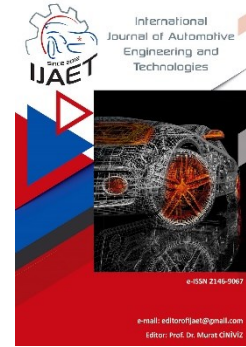


e-ISSN: 2146 - 9067

International Journal of Automotive Engineering and Technologies

journal homepage:

<https://dergipark.org.tr/en/pub/ijaet>



Original Research Article

Stability analysis of an active electromagnetic actuating suspension system



Patrick Olayiwola^{1,*}, Patrick Olabisi²

¹University of Lagos, Department of Systems Engineering, Akoka, Nigeria.

²Bells University of Technology, Department of Electrical, Electronic and Computer Engineering, Ota, Nigeria.

ARTICLE INFO

Orcid Numbers

1. 0000-0002-6714-2789

2. 0000-0001-6414-4431

Doi: 10.18245/ijaet.886129

* Corresponding author
psolayiwola@unilag.edu.ng

Received: Feb 24, 2021

Accepted: Mar 30, 2022

Published: 01 July 2022

Published by Editorial Board
Members of IJAET

© This article is distributed by
Turk Journal Park System under
the CC 4.0 terms and conditions.

ABSTRACT

For Vehicle suspension systems, needs for high force density and ease of design made hydraulic actuating systems commercially viable but inefficient, with bandwidth requirement very small. With active electromagnetic suspension system, the lapse of providing adequate bandwidth is compensated. The governing differential equations of displacement interactions in both spatial and time domains were used and CEFLT algorithms employed in the stability analysis. An optimum for reduction of the electromagnetic actuating force acts as trade-off for given vehicle-road terrain parameters. System instability occurs when the value is decreased and stability is maintained when increased.

Keywords: Vehicle suspension system, bandwidth, CEFLT algorithms, electromagnetic actuating force.

1. Introduction

Effective suspension systems should be able to provide trade-offs between the safe handling, maximum traction and passenger comfort. For this to be achieved, modern suspension systems rely on various types of springs, shock absorbers, control arms, and other components like actuators, sensors, etc. For any type of suspension system used on the vehicle, however, the tires should be made to rise and fall, relative to the body. It must be able to allow the springs and shocks to reduce bumps and road shock, and that the suspension is able to allow the springs and shocks to absorb the energy of a bump for a smooth ride while not allowing uncontrolled movement of the tyres. The suspension is to handle movements caused by vehicle acceleration, braking, and cornering.

The spring must be able to safely carry the weight of the vehicle, since the failure of a spring does not only affect the ride height for the cornering of the vehicle, the spring's ability to carry weight will now be gone, thus resulting in a very rough road ride and increase in the loads and stresses placed on other components [1-3]. Irrespective of the type, suspension system carries the weight of the vehicle. Through the springs and other suspension components, the weight of the vehicle and its occupants is transferred to the wheels and tyres. Not only is the vehicle weight a load, but the additional forces of cornering, braking, accelerating, and negotiating every bump and dips in the road are applied to the suspension and tires. Engineers must balance weight carrying, ride control, comfort and handling when a vehicle is being

designed.

The role of suspension in an all-terrain vehicle can be broadly classified as performance-oriented (handling) and comfort-oriented (ride). The comfort oriented goals include isolation of shocks and vibration from road undulations and performance-oriented goals are to maintain durability, agility and speed of the vehicle on all kinds of challenging terrains. Vehicle vibration which affects ride comfort and vehicle body acceleration was studied in [4, 5].

The design of linear H-infinity suspension controllers served for robust control was used to achieve an optimal control system. A multi-objective uniform-diversity genetic algorithm (MUGA) was used with a diversity preserving mechanism for Pareto optimization of 5-degree-of-freedom vehicle vibration model in [6] to address vehicle constraints such as vertical acceleration of seat, vertical velocity of forward tire, vertical velocity of rear tire, relative displacement between sprung mass and forward tire and relative displacement between sprung mass and rear tire.

Due to the high force density, ease of design, maturity of technology, and commercial availability of the various parts, hydraulic systems are commonly used in body control systems. There is the example of antiroll control (BMW-ARC) system developed by BMW and achieved by placing a hydraulic rotary actuator in the center of the antiroll bar at the rear of the vehicle [7].

All commercial body control systems use hydraulics to provide the active suspension system to improve vehicle roll behavior and ride control. However, the system is still considered inefficient due to the required continuously pressurized system, relative high system time constant (pressure loss and flexible hoses), environmental pollution due to hose leaks and ruptures, where hydraulic fluids are toxic, and mass and intractable space requirements of the total system, including supply system, even though it mainly contributes to the sprung mass. In fact, hydraulic systems have already proved their potential in commercial systems with regard to active roll control (ARC) since the bandwidth requirement is very small (order of hertz), but concerning reduction of road vibrations, the performance of the hydraulic system is insufficient [8].

Thus, with electromagnetic suspension system, the disadvantages of a hydraulic system can be taken care of. This is as a result of the system producing a relatively high bandwidth (tens of hertz), and there is no need for continuous power, ease of control, and absence of fluids. Linear motion can be achieved by an electric rotary motor with a ball screw or other transducers to transform rotary motion to linear translation. However, the mechanism required to make this conversion introduces significant complications to the system. These complications include backlash and increased mass of the moving part due to connecting transducers or gears that convert rotary motion to linear motion (enabling active suspension). More important, they also introduce infinite inertia, and therefore, a series suspension, e.g., where electromagnetic actuation is represented by a rotary motor connected to a ball screw bearing, is preferable. These direct-drive electromagnetic systems are more suited to a parallel suspension, where the inertia of the actuator is minimized [9].

Meanwhile, the cited papers and most other ones in literature present various models ranging from those representing passive as well as semi-active and active suspension systems. The actuating force is either generated by hydraulic, pneumatic or even electromagnetic system, but usually fixed to both the sprung and unsprung masses; however, the suspension system proposed in this paper is only attached to the unsprung mass component of the quarter part of a four wheel vehicular system.

Also, majority of control analysis used in previous papers are based on artificial intelligence (AI) and mainly not considering the spatial domain of balancing change in force requirement of the actuator. Our proposed system takes into account the wave requirement of generating the needed electromagnetic actuating force and, applies complex exponential Fourier-Laplace transforms (CEFLT) solution technique to analyses the problem.

All of the components of the suspension system must work together to provide the proper ride quality and handling characteristics expected by the driver and passengers. Each component is engineered to work as a part of the overall system. If one part of the system fails, it can lead

to faster wear or damage to other components. Therefore, a complete understanding of each component and how it functions as part of the whole suspension system is critical.

This article introduces the stability analysis of the active electromagnetic suspension system, and the section that follows presents the theory of the suspension system with subsections modelling the static configuration, the actuator's force generation and dynamics of the system. Following that, are the sections of stability analysis, results and discussion, conclusion and lastly the references.

2. Theory of the Suspension System

A suspension system carries the weight of the vehicle and serves the purpose of providing proper car handling and comfort of the occupants. By means of the springs and other suspension components, the total weight of a vehicle and its occupants is transferred to the wheels and tyres. The mechanisms of a magnetically-supported active suspension system are shown schematically in Fig 1. These comprises of an assembly of springs, shock absorbers, an actuator and linkages that connects a vehicle to its wheels. The tyre-road reaction per unit depth is signaled by a sensor and transmitted to the electromagnetic actuator for an action.

2.1. Static of suspension system

When a car is stopped or parked at a spot, the suspension mechanism will work so as to provide a balance for the vehicle. In this case, the free-body diagram of the quarter part of the vehicle is as shown in Fig 2. The magnetic actuator works to compensate for the loss of comfort and control that result from a wheel side that enters into a gallop or a pothole. It is the weight of the wheel and suspension components that travels into the pothole or climbs onto the bump-hill. Therefore, the governing equation for the system in its static equilibrium is given by:

$$\begin{aligned}
 k_1(y_1 - y_2) &= m_1 g \\
 (k_2 + k_1)y_2 - k_1 y_1 + F_a y_2' &= m_2 g - Rz \\
 \forall t \leq 0
 \end{aligned}
 \tag{1}$$

where, are spring and tyre stiffness constants respectively,

c_1, c_2 are damping coefficients of the shock

absorber and the tyre respectively,

y_1, y_2 Displacements of the quarter body parts' sprung and unsprung masses respectively,

m_1, m_2 Quarter body masses of sprung and unsprung bodies respectively,

F_a Electromagnetic actuating force,

R Tyre reaction per depth against the road profile,

z Wheel displacement as a result of the road profile

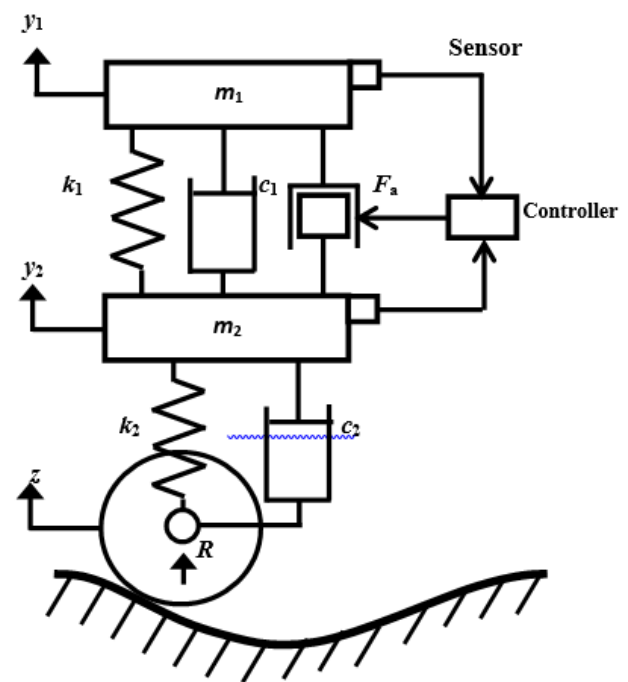


Figure 1: Schematic diagram of a magnetically-actuated active suspension system.

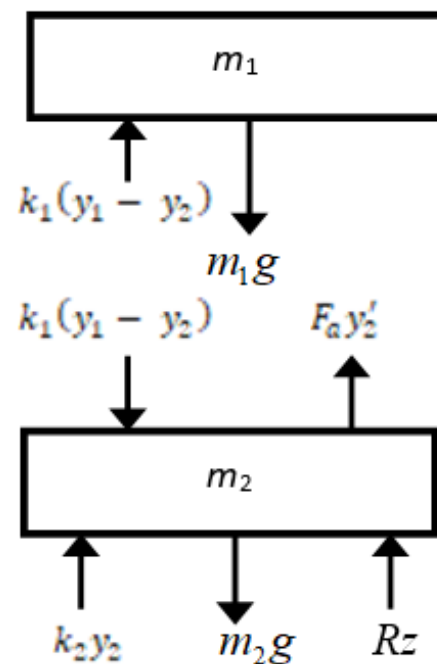


Figure 2: Free-body diagram of the static forces of a quarter part when the vehicle is stationary.

It can be observed that from Eqn. (1), the quarter weight of the car body is taken care of by the spring while that of the unsprung mass is cared for by tyre springs and the levitating force from the actuator. The system generates electromagnetic fluxes required to raise the vehicle's unsprung masses at the affected quarter side.

2.2. Analysis of actuator's force

In a magnetic or electromagnetic system, \mathbf{B} denotes the magnetic flux density, while the magnetic flux Φ_m is expressed by [10]:

$$\Phi_m = \oint \mathbf{B} \cdot d\mathbf{S} \quad (2)$$

If a positive test charge q moving with a velocity v through a point in the magnetic field experiences a deflecting force, \mathbf{F}_m , then, the force due to the magnetic field is given by:

$$\mathbf{F}_m = q \cdot \mathbf{v} \times \mathbf{B} \quad (3)$$

When the velocity of the moving charge is inclined at an angle θ with the magnetic field intensity, Eqn. (3) becomes:

$$F_m = qvB \sin \theta \quad (4)$$

Passing current I through the conductor of length l , and $q = I \cdot dt$, $v = \frac{dl}{dt}$, therefore, Eqn.

(4) can be written as:

$$F_m = BIl \sin \theta \quad (5)$$

As the system can be arranged in such that the magnetic force for the actuator produces maximum values, i.e., when $\theta = \frac{\pi}{2}$, then the work done by the actuator force in lifting or lowering the unsprung mass of the suspension system can be given by:

$$W_a = BIl \cdot dy_2 = F_a \cdot dy_2 \quad (6)$$

and W_a lifts or lowers the actuator's sleeve or piston with a displacement dz , hence, the actuating force F is given by:

$$F = F_a \frac{dy_2}{dz} \quad (7)$$

2.3. Dynamic of suspension system

The free-body diagram of the suspension system during motion is now considered and shown in

Figure 3. This comprises of the inertia, the damping, spring and actuating forces. The arrangement is that of a two - degree-of-freedom system and, the governing equations of motion can be given by:

$$\begin{aligned} m_1 \ddot{y}_1 + c_1(\dot{y}_1 - \dot{y}_2) + k_1(y_1 - y_2) &= 0 \\ m_2 \ddot{y}_2 + c_2 \dot{y}_2 + k_2 y_2 - c_1(\dot{y}_1 - \dot{y}_2) - \\ k_1(\dot{y}_1 - \dot{y}_2) + F_a y_2' &= -Rz \quad \forall t > 0 \end{aligned} \quad (8)$$

subject to Eqn. (1) the initial conditions:

$$\begin{aligned} y_1(z, 0) = f(z) \\ y_2(z, 0) = g(z) \end{aligned} \quad \forall -a \leq z \leq a \\ \dot{y}_1(z, 0) = \dot{y}_2(z, 0) = 0 \quad \forall -a < z < a \\ t \leq 0 \quad (9)$$

and, the following boundary conditions;

$$\begin{aligned} y_1(a, t) = 0 \\ y_2(\pm a, t) = \pm a \end{aligned} \quad \left. \vphantom{\begin{aligned} y_1(a, t) = 0 \\ y_2(\pm a, t) = \pm a \end{aligned}} \right\} \quad \text{at } t > 0 \quad (10)$$

where C is determined by the quarter weight of the car and the stiffness constant of spring.

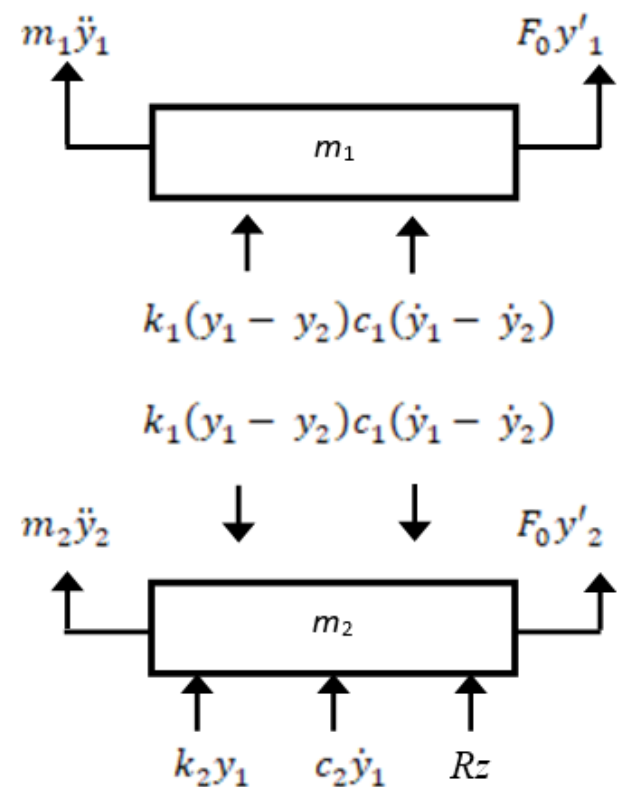


Figure 3: Free-body diagram of forces

3. Stability Analysis

In this section, the complex exponential Fourier-Laplace transforms (CEFLT) algorithms [11] is to be used in analysing the system in its frequency domain. In this respect, the initial and boundary conditions are not assumed but deduced from the governing differential equations (1). Therefore, the integral transforms

are defined as follows:

If,

$$Y_i(\eta, s) = \mathfrak{F}\{y_i(z, t)\} = \int_0^\infty \int_{-a}^a y_i(z, t) e^{-(st-i\eta z)} dz dt \quad (11)$$

then,

$$y_i(z, t) = \mathfrak{F}^{-1}\{\bar{Y}_i(\eta, s)\} = \int_0^\infty \int_{-a}^a \bar{Y}_i(\eta, s) e^{(st-i\eta z)} ds d\eta \quad (12)$$

where

$$\mathfrak{F}^{-1}\{\bar{Y}_i(\eta, s)\} = \begin{cases} Y_i(z, s) & -a \leq z \leq a \\ 0 & z < -a, z > a \end{cases} \quad (13)$$

$i = 1, 2$

3.1. Analysis of initial and boundary conditions

Recall from Eqn. (1) which can be written in matrix form as,

$$\begin{pmatrix} k_1 & -k_1 \\ -k_1 & k_1 + k_2 \end{pmatrix} \begin{pmatrix} y_1 \\ y_2 \end{pmatrix} + \begin{pmatrix} 0 & 0 \\ 0 & F_a \end{pmatrix} \begin{pmatrix} y_1' \\ y_2' \end{pmatrix} = \begin{pmatrix} m_1 g \\ m_2 g - Rz \end{pmatrix} \quad (14)$$

where $y_i = y_i(z'0) \forall i = 1, 2$. On applying Eqns. (11) and (12) to Eqn. (14) and solving

$$y_2(z, 0) = \begin{cases} \{(m_1 + m_2)g/k_2\} \left(1 - e^{-\frac{k_2 z}{F_a}}\right), & \forall z < -a, z > a, t \leq 0 \\ \left\{ \left(\{(m_1 + m_2)g/k_2\} + (2R/k_2) \sinh(ak_2/F_a) \{a - (F_a/k_2)\} \right) \left(1 - e^{-\frac{k_2 z}{F_a}}\right) + \frac{2zR}{k_2} \sinh(ak_2/F_a) \right\} & \forall -a \leq z \leq a, t = 0 \end{cases} \quad (16)$$

$$\bar{Y}_1(\eta, s) = \frac{\{m_2 s^2 + (c_1 + c_2)s + (k_1 + k_2) - iF_a \eta\} G_1 + (c_1 s + k_1) G_2}{(m_1 s^2 + c_1 s + k_1) \{m_2 s^2 + (c_1 + c_2)s + (k_1 + k_2) - iF_a \eta\} - (c_1 s + k_1)^2} \quad (17)$$

$$\bar{Y}_2(\eta, s) = \frac{(m_1 s^2 + c_1 s + k_1) G_2 + (c_1 s + k_1) G_1}{(m_1 s^2 + c_1 s + k_1) \{m_2 s^2 + (c_1 + c_2)s + (k_1 + k_2) - iF_a \eta\} - (c_1 s + k_1)^2} \quad (18)$$

where

$$G_1 = (m_1 s + c_1) \bar{y}_1(\eta, 0) + c_1 \bar{y}_2(\eta, 0) + m_1 \dot{\bar{y}}_1(\eta, 0)$$

$$G_2 = c_1 \bar{y}_1(\eta, 0) + (m_2 s + c_1 + c_2) \bar{y}_2(\eta, 0) - i2 \left\{ a \left(\frac{R}{\eta} - F_a \right) \cos \eta a + \frac{R \sin \eta a}{\eta^2} \right\}$$

Eqns. (17) and (18) are further expanded to give,

simultaneously, the response signals in the spatial domain, are given by:

$$y_1(z, 0) = y_2(z, 0) + \frac{m_1 g}{k_1} \quad (15)$$

and see Eqn. (16).

From Eqn. (15), it can be seen that when the actuator's sleeve z is on the zero mark (i.e. $z = 0$), displacement signal $y_1(z, 0)$ is a sole product of comparing the weight of the car body with the spring constant of the suspension spring for the quarter side under consideration. This is showing that the sprung spring k_1 is the component that is supporting the car body at rest. From Eqn. (16), however, the displacement signal $y_2(z, 0)$ has limiting values of $z = \pm a$ and with $z = 0$, $y_2(z, 0) = 0$.

3.2 Analysis of the dynamic model of suspension system

The response of the suspension system as the vehicle tours a road terrain as described by the governing equations can now be determined on applying Eqns. (11) and (13) to Eqn. (8), and solving the system simultaneously. The resulting displacement signals in the frequency domains for both sprung and unsprung masses are given as (17) and (18).

$$\bar{Y}_1(\eta, s) = \frac{\left\{ \begin{aligned} &(s^3 + \alpha_1 s^2 + \alpha_2 s + \alpha_3) \bar{y}_1(\eta, 0) + (\alpha_4 s^2 + \alpha_5 s + \alpha_6) \bar{y}_2(\eta, 0) \\ &-i \frac{2(c_1 s + k_1)}{m_1 m_2} \left\{ a \left(\frac{R}{\eta} - F_a \right) \cos \eta a + \frac{R \sin \eta a}{\eta^2} \right\} \end{aligned} \right\}}{D} \quad (19)$$

and

$$\bar{Y}_2(\eta, s) = \frac{\left\{ \begin{aligned} &(s^3 + \gamma_1 s^2 + \gamma_2 s + \gamma_3) \bar{y}_2(\eta, 0) + (\gamma_4 s^2 + \gamma_5 s + \gamma_6) \bar{y}_1(\eta, 0) \\ &-i \frac{2(m_1 s^2 + c_1 s + k_1)}{m_1 m_2} \left\{ a \left(\frac{R}{\eta} - F_a \right) \cos \eta a + \frac{R \sin \eta a}{\eta^2} \right\} \end{aligned} \right\}}{D} \quad (20)$$

where

$$\begin{aligned} \bar{y}_1(\eta, 0) &= \bar{y}_2(\eta, 0) + \frac{m_1 g}{\eta k_1} \sin \eta a \\ \bar{y}_2(\eta, 0) &= \left\{ \frac{(m_1 + m_2)g}{k_2} + \frac{4R}{k_2} \left(a - \frac{F_a}{k_2} \right) \sinh \left(\frac{ak_2}{F_a} \right) \right\} \left\{ \frac{\sin \eta a}{\eta} - i \frac{F_a}{k_2 - i\eta F_a} \sin \left(\frac{k_2 - i\eta F_a}{F_a} a \right) \right\} \\ &\quad + \frac{4R}{\eta k_2} \left(a + i \frac{1}{\eta} \right) \sin \eta a \sinh \left(\frac{ak_2}{F_a} \right) \\ \alpha_1 &= \frac{m_2 c_1 + m_1 (c_1 + c_2)}{m_1 m_2}; \alpha_2 = \frac{c_1 (2c_1 + c_2) + m_1 (k_1 + k_2) - im_1 \eta F_a}{m_1 m_2}; \\ \alpha_3 &= \frac{c_1 (2k_1 + k_2 - i\eta F_a)}{m_1 m_2}; \alpha_4 = \frac{2c_1}{m_1}; \alpha_5 = \frac{2c_1 (c_1 + c_2) + m_2 k_1}{m_1 m_2}; \\ \alpha_6 &= \frac{c_1 (2k_1 + k_2 - i\eta F_a) + k_1 c_2}{m_1 m_2} \\ \gamma_1 &= \frac{m_1 (2c_1 + c_2) + m_2 c_1}{m_1 m_2}; \gamma_2 = \frac{c_1 (2c_1 + c_2) + c_1 k_1 + m_2 k_1}{m_1 m_2}; \\ \gamma_3 &= \frac{k_1 (2c_1 + c_2)}{m_1 m_2}; \gamma_4 = \frac{2c_1}{m_2}; \gamma_5 = \frac{2c_1^2 + m_2 k_1}{m_1 m_2}; \gamma_6 = \frac{2c_1 k_1}{m_1 m_2} \\ \left. \begin{aligned} &\beta_1 = \frac{(m_1 + m_2)c_1 + m_1 c_2}{m_1 m_2}; \beta_2 = \frac{(m_1 + m_2)k_1 + m_1 k_2 + c_1 c_2 - im_1 F_a \eta}{m_1 m_2}; \\ &\beta_3 = \frac{c_1 k_2 + k_1 c_2 - ic_1 F_a \eta}{m_1 m_2}; \beta_4 = \frac{k_1 (k_2 - iF_a \eta)}{m_1 m_2} \\ &D = s^4 + \beta_1 s^3 + \beta_2 s^2 + \beta_3 s + \beta_4 \end{aligned} \right\} \quad (23)$$

Table 1: Values of suspension parameters

Parameters	Iron	Nylon
m_1	450 kg	Sprung mass
m_2	40 kg	Unsprung mass
k_1	30 kN/m	Spring stiffness
k_2	160 kN/m	Tyre stiffness
c_1	2k Ns/m	Shock damping coefficient
c_2	15 kNs/m	Tyre damping coefficient

4. Result and Discussion

Firstly, analysis of the system's static or initial configuration in spatial domain (while time $t=0$) i.e. before it is excited to move, is considered. In this case, it is possible that the vehicle is parked with any of its wheels inside a pothole or on a raised bump. The unsprung mass components are assumed to be flexible enough so as to maintain a comfortable standing position of the vehicle's body. Secondly, the dynamic system

of the suspension mechanism is analysed in the frequency domains, to determine its stability. This is important because the actuating force is allowed to control only the unsprung mass without touching the sprung mass directly.

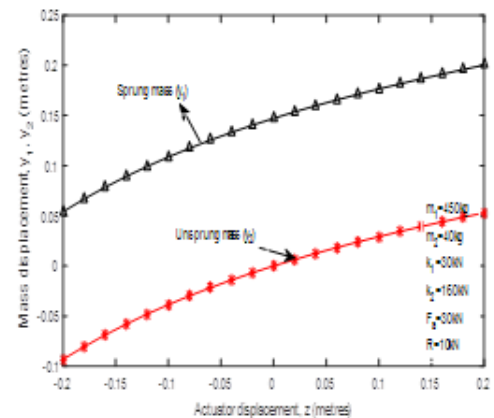
4.1 Result of the static analysis

Depending on the parking condition of the vehicle, a wheel that is not parked on a levelled surface will demand a measurable amount of force to keep it balanced. And as shown in Fig 4, the car parked (at $t = 0$) on a levelled ground i.e. when $z = 0$ returns zero deflection of the unsprung mass (i.e. $y_2(z) = 0$). However, the case is different with the sprung mass deflection since the spring does the work of carrying the weight of the vehicle. Figure 4(a) demonstrates almost linear relationship between the deflection of the masses and actuator displacements when the range of values of the actuator's sleeve is closer. It means that the space between the levelled ground and the tyre centre is low. On another hand, a departure of linear relations between z and $y_2(z)$ is illustrated by Figure 4(b) as the range of values of z increases for the given parameter. The range of z for which Figures 4(a) and 4(b) were plotted are given for (a) as $-0.2 < z < 0.2$ and for (b) as $-0.3 < z < 0.3$.

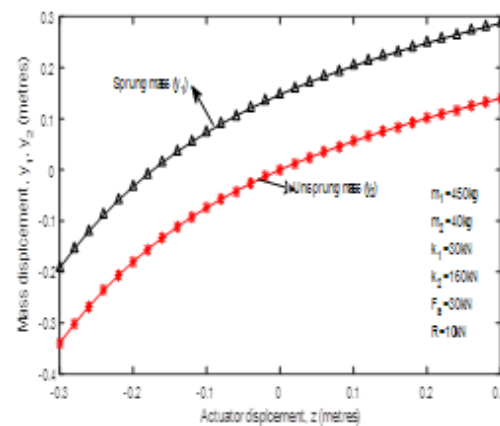
4.2 Result of the dynamic analysis

The results of the stability analysis of the active electromagnetic actuating suspension system are presented. Illustrated in Figure 5(a) is the resonance occurrence at the lower system frequency with the sprung mass dynamics and stability of the body is sustained. It is demonstrated that the system responds quickly to any change on road terrain except with a situation of a longer stay that may make the vehicle frequency equal to one of system natural frequencies. Comparing a hydraulic actuating active system which has the limitation of producing a narrow bandwidth, the electromagnetic actuator generates enough bandwidth as depicted by the magnitude response in Figure 5(b). In this case the curve produces flat top, therefore generating a wider bandwidth. Figures 5(c) and 5(d) show the phase responses of the vehicle body and suspension system dynamics, respectively. Stability is

supported with the phase angle decreasing and its values remaining between 0 and $-\pi$ as the frequency of the system increases.



a. For $-0.2 < z < 0.2$



b. For $-0.3 < z < 0.3$

Figure 4: Varying the actuator displacement bounds.

Vehicle body dynamics is essentially observed for stability, as its unstable conditions will create discomfort for passengers and damage to some delicate loads. Thus, Figure 6 depicts the Nyquist Plot for the sprung and unsprung mass systems and, a fine selection of parameters such that both the vehicle body (\bar{Y}_1) and the suspension (\bar{Y}_2) displacements are on stable pedestals. Although, for the given value of road-wheel reaction, stability can be optimized further by varying the value of the electromagnetic actuating force.

Figure 7 shows that the system may not be accepted to be stable, even though the suspension unit of it appears stable as shown in Figure 7(b). In Figure 7(a), the vehicle body is unstable; also the curve demonstrates the narrowing of the bandwidth as a result of trying to drive the actuator with a smaller amount of force. This is an important area too as greater force value requires higher no of turns of coil,

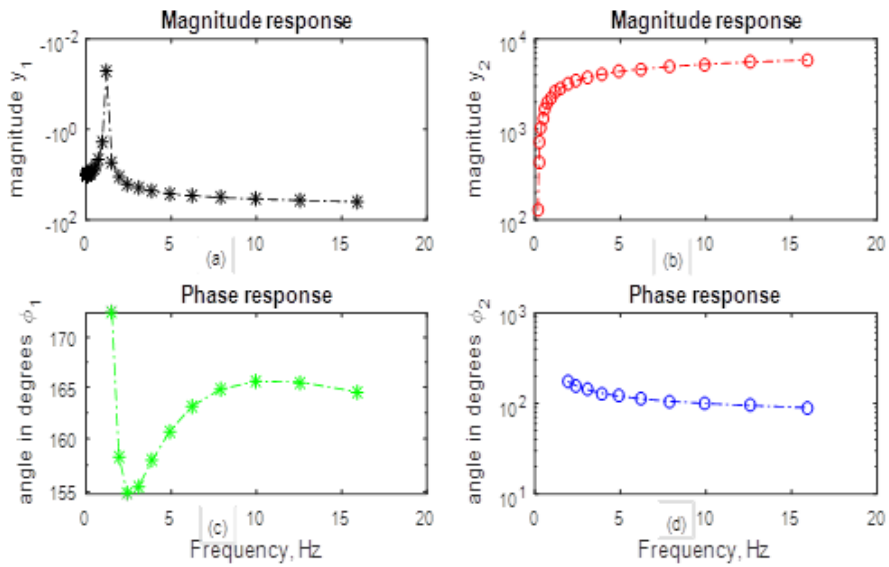


Figure 5: Magnitude and phase responses with $a = 0.3m$, $F_a = 15.3kN$, $R = 20kN/m$

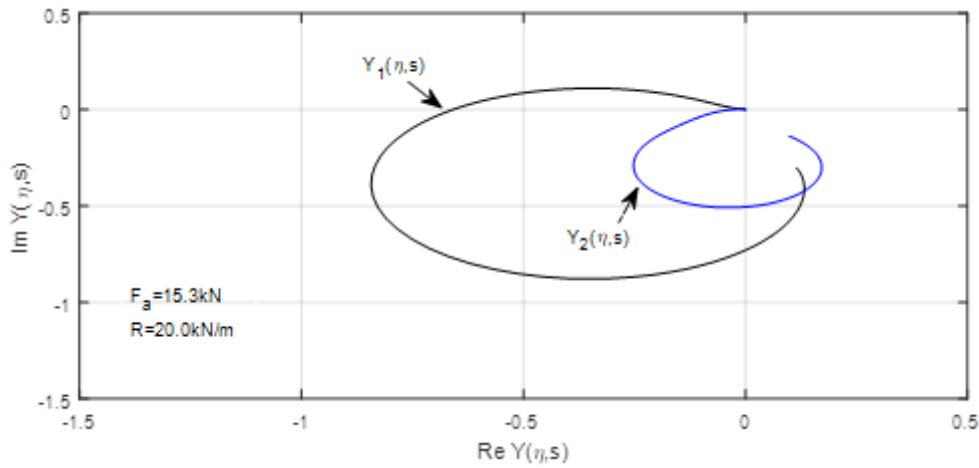


Figure 6: Nyquist Plots of $Y_1(\eta, s)$ and $Y_2(\eta, s)$

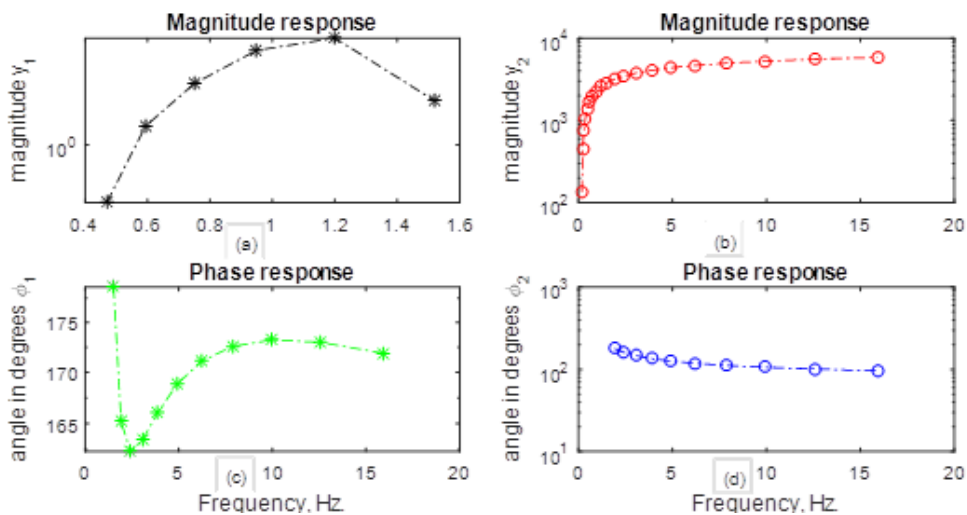


Figure 7: Magnitude and phase responses with $a = 0.3m$, $F_a = 13.3kN$, $R = 20kN/m$

which in turn increases the weight of the device. While the phase angles in Figures 7(c) and (d) are similar to those of Figures 5(c) and (d), the reality is that the system is not stable. This

condition is further proved by showing with the system's Nyquist Plot of Figure 8 that sprung mass dynamics turns out to become an unstable system. The cross-over frequency of the curve

for that vehicle body part of the system has actually enclosed point $(-1 + j0)$, a condition for instability. However, the suspension system demonstrates stability since it crosses the negative real-axis before the point. In this case, handling may be possible but passengers' comfort has been distorted, hence there is a need for proper trade-off in the analysis.

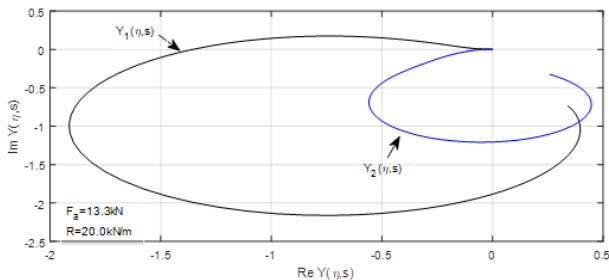


Figure 8: Nyquist Plots of $Y_1(\eta, s)$ and $Y_2(\eta, s)$

5. Conclusion

The stability analysis of an active electromagnetic suspension system has been investigated in this paper. It is found that wider bandwidth is needed for effective active suspension system in a vehicle. This is possibly provided by the use of an electromagnetic actuator, other than a hydraulic actuator that only provides larger actuating force but narrow bandwidth. It is also discovered that to optimize system stability, the electromagnetic actuating force can be varied for ranges of values of road-wheel reaction for any given vehicle suspension parameters. Acceptable stability points are determined on frequency response and Nyquist Plots.

CRedit authorship contribution statement

Olayiwola: Conceptualization (lead); literature review (lead); mathematical and results analyses; software graphics; validation.

Olabisi: Conceptualization (supporting); literature review (supporting); figures design; review and editing; draft preparation and correspondence. Both authors read and approved of the final manuscript.

Declaration of Competing Interest

There are no competing interests to this article found anywhere.

Statement of Support and Acknowledgment:

No support, whether financial or material

support, was received from anyone or any institution in the course of this research work and publication.

Nomenclature

- k_1 : Spring stiffness constant,
- k_2 : Tyre stiffness constant,
- c_1 : Damping coefficient of the shock absorber,
- c_2 : Damping coefficient of tyre,
- y_1 : Displacement of the quarter parts of the sprung mass,
- y_2 : Displacement of the quarter part of the unsprung mass,
- m_1 : Quarter body mass i.e. the sprung mass,
- m_2 : Quarter mass of the unsprung bodies,
- F_a : Electromagnetic actuating force,
- R : Tyre reaction per depth against the road profile,
- z : Wheel displacement on the road profile,
- Φ_m : Magnetic flux,
- \mathbf{B} : Magnetic field vector,
- \mathbf{F}_m : Deflecting force vector,
- W_a : Work done by the actuator
- CEFLT** : Complex Exponential Fourier-Laplace Transforms
- MUGA** : Multi-objective Uniform-diversity Genetic Algorithm
- ARC** : Active Roll Control

6. References

1. Jain, K. K. and Asthana R. B., "Automobile Engineering", Tata McGraw-Hill, London, 293-294, 2002.
2. _____, "Suspension System Principles", Cengage Learning, 175-200, 2014.
3. Fenton, J., "Handbook of vehicle design analysis", Society of Automotive Engineers, 151-282, 1976.
4. Liu, Y., "Recent Innovations in Vehicle Suspension Systems". Recent Patents on Mechanical Engineering, Vol 1, No 3, 206-210, 2008.
5. Sepehri, B. and Hemati, A., Active Suspension vibration control using Linear H-Infinity and Optimal Control. International Journal of Automotive Engineering Vol. 4, No 3, 805-811, Sept 2014.
6. Salehpour, M., Jamali, A. and Nariman-zadeh, N. "Optimal Selection of Active

Suspension Parameters Using Artificial Intelligence”. International Journal of Automotive Engineering Vol. 1, No. 4, 244-255, October 2011.

7. Strassberger M. and J. Guldner J., “BMW’s dynamic drive: An active stabilizer bar system,” IEEE Control Syst. Mag., Vol. 24, No. 4, 28–29, Aug. 2004, 107.

8. Gysen, B.L.J., Paulides, J.J.H., Janssen, J.L.G. and Lomonova, E. “Active electromagnetic suspension system for improved vehicle dynamics”. IEEE Transactions on Vehicular Technology, Vol 59, No. 3, 1156-1163, March 2010.

9. Xue X. D., Cheng K. W. E., Zhang Z., Lin J. K., Wang D. H., Bao Y. J., Wong M. K., and Cheung N. “Study of Art of Automotive Active Suspensions”. 4th International Conference on Power Electronics Systems and Applications, 2011.

10. Gaur R.K. and Gupta S.L. Engineering Physics, Dhanpat Rai Publications (P) Ltd., New Delhi, Reprinted 8th Edition, 47.1-2, 2005.

11. Olunloyo V.O.S., Osheku C.A. and Olayiwola P.S. “A Note on an Analytic Solution for an Incompressible Fluid-Conveying Pipeline System”. Advances in Acoustics and Vibration, Vol. 2017, Article ID 8141523, 2017.